ACS OMEGA

http://pubs.acs.org/journal/acsodf

Article

Diverse Pathway to Obtain Antibacterial and Antifungal Agents Based on Silica Particles Functionalized by Amino and Phenyl Groups with Cu(II) Ion Complexes

Veronika V. Tomina, Iryna M. Furtat, Anastasia P. Lebed, Sofiya S. Kotsyuda, Hristo Kolev, Maria Kanuchova, Dominika Marcin Behunova, Miroslava Vaclavikova, and Inna V. Melnyk*

Cite This: *ACS Omega* 2020, 5, 15290−15300

Read Online

ACCESS | Metrics & More | Article Recommendations | Supporting Information

ABSTRACT: Production of environmentally friendly multitasking materials is among the urgent challenges of chemistry and ecotechnology. The current research paper describes the synthesis of amino−/silica and amino−/phenyl−/silica particles using a one-pot sol−gel technique. CHNS analysis and titration demonstrated a high content of functional groups, while scanning electron microscopy revealed their spherical form and ∼200 nm in size. X-ray photoelectron spectroscopy data testified that hydrophobic groups reduced the number of water molecules and protonated amino groups on the surface, increasing the portion of free amino groups. The complexation with Cu(II) cations was used to analyze the sorption capacity and reactivity of the aminopropyl groups and to enhance the antimicrobial action of the samples.

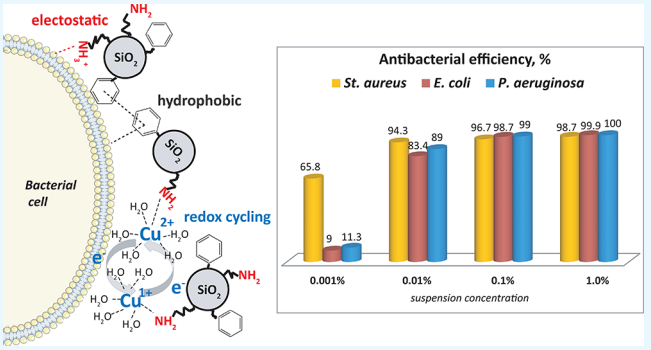

Antibacterial activities of suspensions of aminosilica particles and their derivative forms containing adsorbed copper(II) ions were assayed against Gram-positive (*Staphylococcus aureus* ATCC 25923) and Gram-negative bacteria (*Escherichia coli* ATCC 25922 and *Pseudomonas aeruginosa* ATCC 27853). Meanwhile, antifungal activity was tested against fungi (*Candida albicans* UCM Y-690). According to zeta potential measurements, its value could be depended on the suspension concentration, and it was demonstrated that the positively charged suspension had higher antibacterial efficiency. SiO_2/−C_6H_5/−NH_2 + Cu(II) sample's water suspension (1%) showed complete growth inhibition of the bacterial culture on the solid medium. The antimicrobial activity could be due to occurrence of multiple and nonspecific interactions between the particle surfaces and the surface layers of bacteria or fungi.

INTRODUCTION

Recently, the scientific community has been facing a challenging task of creating antimicrobial agents and technologies without triggering undesirable microbial resistance.[1,2] The solution of such a task requires multidisciplinary effort because the devices and materials designed for therapeutic purposes should also possess antimicrobial and/or antifungal properties. Moreover, the researchers are getting more interested in contact-active biocidal materials killing the bacteria via direct interaction with bacterial cell walls rather than releasing biocides.[3]

Among others, silica-based materials, especially, functionalized silica nanoparticles have attracted the attention of the researchers in terms of their antimicrobial properties.[3,4] Such functionalized silica-based nanoparticles are widely used in numerous fields of science, including controlled delivery of organic and inorganic molecules and, what is also important, were shown to improve the antibacterial effect of most therapeutic agents.[5] Their advantages include biocompatibility, low cytotoxicity, controllable particle size, and adjustable surface properties.[6] There are several instruments for increasing the antibacterial action of nanoparticles. One of them is introducing specific functions onto their surface which would determine their physicochemical properties. According to Mathelié-Guinlet et al.,[7] pure silica nanoparticles exhibit a microbicidal effect when their critical diameter is under 50 nm. However, the antibacterial action of functionalized particles, especially positively charged, is less size-dependent and mainly connected with their privileged electrostatic affinity to negatively charged bacterial cell walls. Numerous publications describe antibacterial properties of silica particles functionalized with N-containing groups, polymers,[8−10] and antibiotics,[11] determined by their positive surface charge. Antimicrobial performance can improve with the increasing

Received: March 25, 2020
Accepted: June 2, 2020
Published: June 16, 2020

Table 1. Synthesis Conditions and Properties of Mono- and Bifunctional Silica Nanoparticles

sample	N, mass (%)	C, mass (%)	H, mass (%)	concentration of NH_2- groups (mmol g^{-1})			concentration of C_6H_5- groups (mmol g^{-1})		SC to Cu(II) (mmol g^{-1})
				theor. data	elem. anal. data	titr. data	theor. data	elem. anal. data	
NH_2-/SiO_2	3.42	8.91	2.97	3.3	2.4	2.0	0	0	1.0
$NH_2-/C_6H_5-/SiO_2$	3.16	15.9	3.27	1.7	2.3	2.3	1.7	1.1	2.2

number of active sites to interact bacterial cells. For example, Lee et al.[8] showed that the state of the surface amino groups is a key factor in increasing kill-efficiency of the materials. In addition, amino groups from silica can be used for the following immobilization of antimicrobial compounds[12] and ions, for example, of silver[13] and copper.[14,15] Regarding the latter, copper is known to possess excellent antimicrobial properties in various forms, being less studied than silver.[16] Therefore, copper-containing materials have been recently probed for different applications as antimicrobial agents,[16,17] and it was ascertained that incorporating complexes of copper ions is an effective strategy of increasing microbicidal[18,19] and antifungal[20] action of the materials.

Thus, in our research, we synthesized aminosilica particles with potential application in the treatment of sewage waters, including those contaminated with microorganisms. Therefore, we considered it appropriate to carry out screening analysis of the presence/absence of the antimicrobial effect for mono- and bifunctional aminosilica microspheres, NH_2-/SiO_2, and $NH_2-/C_6H_5-/SiO_2$, on the cells of strains of Gram-positive bacteria *Staphylococcus aureus*, Gram-negative bacteria *Escherichia coli*, and *Pseudomonas aeruginosa*, as well as eukaryotic microorganisms on the example of single-cell microscopic fungi *Candida albicans*. Such a choice of test cultures was caused by peculiarities of the chemical composition, structural organization, and cell wall architectonics of different microorganisms, each characterized by specific components. In particular, there are peptidoglycans (PGs), teichoic acids, and lipopolysaccharides in the surface layers of bacteria, while fungi contain mannan and glucan.[21] Aminosilica particles were synthesized via a relatively simple one-stage technique, and additional surface phenyl groups were introduced as inherent to many antimicrobial agents capable of nonspecific interactions with bacterial and fungal cell walls.[22] Derivatives with adsorbed copper(II) ions were also used.

EXPERIMENTAL SECTION

Sample Preparation. *Reagents.* Tetraethyl orthosilicate, $Si(OC_2H_5)_4$ (TEOS, 98%, Aldrich), 3-aminopropyltriethoxysilane, $NH_2(CH_2)_3Si(OC_2H_5)_3$ (APTES, 99%, Aldrich), and phenyltriethoxysilane, $C_6H_5Si(OC_2H_5)_3$ (PhTES, 98%, Aldrich) were purchased. The reaction was conducted in ethanol, C_2H_5OH, (96%, LLC Bio-pharma) and catalyzed with NH_4OH (25%, Lach-Ner). The source of copper(II) ions was $Cu(NO_3)_2{\cdot}3H_2O$ (analytical grade, ITES Vranov, Slovakia).

Procedure of Sample Production. The one-pot approaches described in ref 4, 23 were used to synthesize two types of samples: amino−/silica (NH_2-/SiO_2) and amino−/phenyl−/silica ($NH_2-/C_6H_5-/SiO_2$). Briefly, TEOS (0.018 mol) and APTES (0.006 mol) [or APTES (0.003 mol) with PhTES (0.003 mol)] were mixed with ethanol (100 mL). After opalescence observation (around 30−40 min of constant stirring), ammonia solution (2 mL) was added to the mixture, and the reaction continued for 60 min. The precipitate was separated by centrifugation (15 min, 6000 rpm), washed three times with ethanol to remove nonreacted reagents, and dried at 100 °C for 24 h. The characteristics of the samples are summarized in Table 1.

To obtain samples with copper(II) ions (Cu(II) + NH_2-/SiO_2 and Cu(II) + $NH_2-/C_6H_5-/SiO_2$), a batch of each sample (0.025 g) was poured with 25 mL of 0.02 M copper(II) nitrate solution (pH ≈ 4.9, t = 25 °C. The sorption capacity (SC) of the samples was calculated from the difference in the Cu^{2+} concentration in the solution before and after sorption (Table 1). Before the preparation of test suspensions, the samples were washed with water and dried.

Characterization. The surface morphology and elemental composition of nanoparticles were measured by a field emission scanning electron microscope MIRA 3 (TESCAN, Czech Republic) equipped with a high-resolution cathode (Schottky field emitter), three-lens Wide Field Optics design, and energy-dispersive X-ray detector (EDX) (Oxford Instruments, UK). For analysis, the samples were mounted on a metal stub with adhesive carbon tape, coated with 15 nm of carbon. Conductive carbon coating is necessary to avoid charging artifacts. A method of photon cross-correlation spectroscopy (PCCS) using a Nanophox particle size analyzer (Sympatec, Germany) was employed to determine samples' particle-size distributions.

The CHNS analysis was carried out by the elementary analyzer Vario MACRO cube (Elementar Analysensysteme GmbH, Germany) with a thermal conductivity detector. Helium and oxygen (both purity 99.995%) were used as the carrier and combustion gases, respectively, with the intake pressures of 2 bars. The combustion tube was set up at 1150 °C and reduction tube at 850 °C. Sulfanilamide $C_6H_8N_2O_2S$ (Germany) was used as the CHNS standard. The content of amino groups (C_{amino}, mmol g^{-1}) was calculated from the mass fraction of the element N using the following formula: $C_{amino} = 1000\omega/100m_a = 10\omega/m_a$ (ω—content of nitrogen, %; m_a—atomic mass of nitrogen, g mol^{-1}). The content of phenyl groups (C_{phenyl}, mmol g^{-1}) was calculated from the mass fraction of the element C that does not apply to aminopropyl groups: $C_{phenyl} = (10\omega/m_a - 3C_{amino})/6$ (ω—content of carbon, %; m_a—atomic mass of carbon, g mol^{-1}). The content of amino groups was also determined by acid−base titration.

Diffuse reflectance infrared Fourier transform (DRIFT) spectra were recorded for the samples ground with solid KBr (Spectranal, Aldrich) on a Thermo Nicolet Nexus FTIR spectrometer in the 400−4000 cm^{-1} range.

Zetasizer Nano ZS with DTS1070 cells (Malvern, Great Britain) was used for zeta potential measurements. Each sample (0.05 g) was dispersed into 0.001 M $NaNO_3$ solution (5 mL) by ultrasonication for 10 min (1% suspension). Other concentrations were prepared from 1% suspensions. The results are the average of three independent measurements.

https://dx.doi.org/10.1021/acsomega.0c01335
ACS Omega 2020, 5, 15290−15300

The copper(II) ion concentration in the solutions was measured by atomic absorption spectroscopy (AAS) using a Varian AA 240 FS atomic absorption spectrometer (Australia).

X-ray photoelectron spectroscopy (XPS) measurements were performed on the ESCALAB 2 spectrometer (VG Scientific, UK) with the base pressure inside the analysis chamber maintained at 5×10^{-10} mbar (2×10^{-8} mbar during measurements). The determination was conducted using a twin anode Mg Kα/Al Kα nonmonochromated X-ray source with excitation energies of 1253.6 and 1486.6 eV, respectively. The total instrumental resolution (measured with the FWHM of Ag $3d_{5/2}$ photoelectron line) was 1.06 and 1.18 eV for Mg Kα and Al Kα excitation sources, respectively. The data were analyzed by the software package SpecsLab2 CasaXPS (Casa Software Ltd.). To calibrate the energy scale, the C 1s line of hydrocarbons was normalized to 285.0 eV. The spectra processing included subtraction of X-ray satellites and Shirley-type background.[24] Peak positions and areas were evaluated using the symmetrical Gaussian−Lorentzian curve fitting. The relative concentrations of different chemical species were determined by normalizing the peak areas to their photoionization cross-sections calculated by Scofield.[25]

Antibacterial and Antifungal Tests. *Test Cultures of Microorganisms.* For antibacterial and antifungal tests, we used *S. aureus* ATCC 25923, *E. coli* ATCC 25922, *P. aeruginosa* ATCC 27853, and *C. albicans* UCM Y-690 grown in tryptone soya yeast extract agar (TSA, Himedia, India) for 24 h at 36 ± 1.0 °C in aerobic conditions. The microorganisms were suspended in 0.15 M NaCl solution to reach the turbidity equivalent of 0.5 McFarland standard units (1.5×10^8 cells mL^{-1} for *S. aureus*, *E. coli*, *P. aeruginosa*, and 1.5×10^6 cells mL^{-1} for *C. albicans*) using a densitometer DEN-1 (Biosan, Latvia). These initial standardized suspensions were diluted with saline solution to the concentration of 1.5×10^5 cells mL^{-1} for *S. aureus*, *E. coli*, and *C. albicans* and 1.5×10^4 cells mL^{-1} for *P. aeruginosa*.

Determination of Antimicrobial and Antifungal Activity. Determination of cell viability of *S. aureus*, *E. coli*, *P. aeruginosa*, and *C. albicans* after exposure to silica nanoparticles was performed by the method of macrocultivation seeding of samples on a dense TSA in Petri dishes.[16,26] In order to reveal the antibacterial activity, 200 μL of the bacterial cell suspension was added to the test tubes, containing 1800 μL of the corresponding concentration of silica nanoparticles (1.0, 0.1, 0.01, or 0.001% v). Consequently, we obtained 1.5×10^4 cells mL^{-1} concentrations of *S. aureus*, *E. coli*, and *C. albicans* cells, and 1.5×10^3 cells mL^{-1} concentration of *P. aeruginosa*.

The contact time of the test culture with nanoparticles was τ = 60 and 120 min at 25 ± 1.0 °C (such temperature was chosen for possible future application of the particles in sewage treatment) and constant mixing with a EKROS 6300M shaker at a frequency of 32 min^{-1}. After the contact, 100 μL of each sample was spread on the TSA of two Petri dishes and incubated for 24 h at 36 ± 1.0 °C in aerobic conditions. In 24 h, the grown CFUs (colony-forming units) were calculated, and relative cell viability [survival index (SI)] was estimated. The percentage of inhibited cells was determined from the difference between the living cells in the tested sample with silica nanoparticles and the control (microbial suspension without nanoparticles prepared and grown under the same conditions, set as 100%).

The number of CFUs was calculated as an average of two Petri dishes used in one experiment (n = 1). Each independent experiment and the control were repeated several times depending on the growth of microorganisms. The averaged numerical data were used to calculate average values, their mean square errors, and probability level (p). Because the obtained values did not correspond to the normal distribution and the selection size was small, we used the Kruskal−Wallis test for comparing groups which is a nonparametric alternative to the t-test for independent samples.[27] The number of CFUs (N) was calculated using the formula

$$N = M \cdot R / V$$

where R is the dilution from which cultivation was performed; V is the volume (mL) of the inoculum plated in a Petri dish; and M is the average number of grown colonies.[28]

The CFU (N) values calculated by the formula are hereinafter expressed as lg CFUs mL^{-1}, and they were used to calculate SI (%)

$$SI = N_e / N_c \times 100$$

where indexes N_e and N_c refer to the experimental and control groups (see exact numbers in Table S1).

RESULTS AND DISCUSSION

Structure and Surface Chemistry of Aminosilica Spherical Particles. Amino−/silica and amino−/phenyl−/silica microparticles with and without adsorbed copper(II) ions were chosen for the research. These spherical particles were synthesized via a one-pot procedure in water−ethanolic media using the ammonia catalyst[29] to provide similar particle sizes and amino group contents.

Elemental analysis and acid−base titration data confirm a similar amount of amino groups in both samples (Table 1). The divergence in elemental analysis and titration of NH_2−/SiO_2 may result from the inaccessibility of the groups or their washing off in the acidic medium. As previously reported,[4,23] the presence of additional trifunctional silane with an organic group during the sol−gel transformations of TEOS and APTES affects the speed of co-condensation. There are simultaneous reactions of hydrolysis, condensation, and dissolution proceeding in the alkaline medium created by amino groups.[30] The introduction of additional nonspecific organic groups displaces the equilibrium of the processes in the direction of condensation and formation of inorganic networks with organic groups. Therefore, despite the smaller quantity of APTES used for NH_2−/C_6H_5−/SiO_2 synthesis, both NH_2−/SiO_2 and NH_2−/C_6H_5−/SiO_2 contain identical amounts of amino groups. Also, according to elemental analysis, the groups are not hydrolyzed during the adsorption of copper(II) ions.

The DRIFT spectra of the samples (Figure S1) have all bands characteristic for silica materials with amino groups: two low-intensity absorption bands at 3295 and 3363 cm^{-1} referring to ν_s(NH) and ν_{as}(NH) stretches in amino groups; absorption band at 1593 cm^{-1} corresponding to the $\delta(NH_2)$ vibrations; and the most intensive adsorption band in the region of 1000−1200 cm^{-1} related to ≡Si−O−Si≡ network stretching and bending vibrations. In the DRIFT spectra of amino−/phenyl−/silica samples, there is also a low-intensity adsorption band at 3060 cm^{-1} referring to ν(=C−H) vibrations of phenyl groups. The complex formation on the surfaces of the particles, between amino groups and copper(II) ions, is proved in the DRIFT spectra of the copper-containing samples by the disappearance of the absorption bands of stretching vibrations for amino groups in the region 3290−

https://dx.doi.org/10.1021/acsomega.0c01335
ACS Omega 2020, 5, 15290−15300

3370 cm^{-1}, the band shift of the bending vibrations for amino groups to 1530 cm^{-1}, and the presence of an absorption band at 1350 cm^{-1} corresponding to nitrate ions.

It also should be mentioned that the arrangement of amino groups on the surfaces of these samples varies and is favorable for the formation of complexes with copper(II) ions of different compositions, affecting the values of the static SC (Table 1). Thus, one copper(II) ion interacts with two surface amino groups of NH_2-/SiO_2 and one of $NH_2-/C_6H_5-/SiO_2$. It means that steric difficulties contribute to the simplification of the surface complex between Cu^{2+} and amino groups. The stability of the complex under the conditions of the experiment was confirmed by stirring the sample Cu(II) + $NH_2-/C_6H_5-/SiO_2$ in physiological saline solution for 2 h with verification of the copper(II) ion concentration by AAS. It was shown that under these conditions, the amount of desorbed copper(II) ions is 0.05 mg for 1% suspension.

The SEM images (Figure 1) of NH_2-/SiO_2 and $NH_2-/C_6H_5-/SiO_2$ showed spherical particles about 200 nm in size,

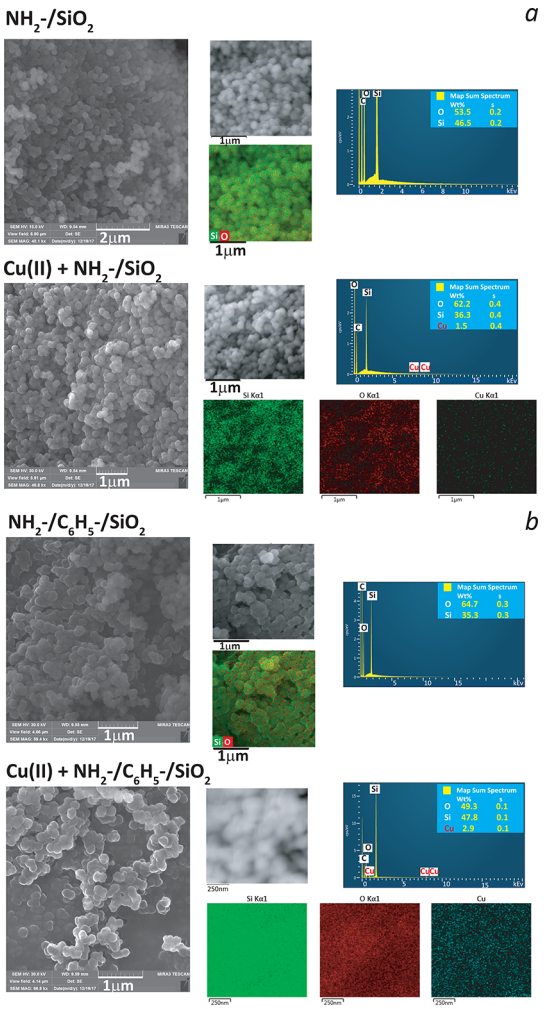

Figure 1. SEM images and EDX analysis of the amino−/silica (a) and amino−/phenyl−/silica (b) samples.

and such a morphology remains after adsorption. Such particle's size was confirmed by particle size distribution analysis (Figure S2). EDX spectra of all samples detected C, O, Si, and Cu (after Cu^{2+} adsorption) and indicate that $NH_2-/C_6H_5-/SiO_2$ uptakes twice more Cu^{2+} than NH_2-/SiO_2.

According to Mathelié-Guinlet et al.,[7] positively charged nanoparticles disrupt bacterial membrane integrity and are more toxic than negatively charged nanoparticles. Therefore, we prepared suspensions with different concentrations of particles (used in the antibacterial tests) and measured their zeta potential and pH values (Table 2). There is a significant difference in the pH values of 1% particles suspensions. They change from alkaline to neutral with Cu^{2+} adsorption. However, the pH values of all diluted suspensions are about 7. Moreover, contrary to the zeta potential, the pH value changes linearly with the dilution of the suspension (Table 2).

Electrokinetic potential is a very complicated phenomenon depending on such factors as pH, ionic strength, valency of the ions, concentration, types of interactions on the surface, and so forth. The zeta potential value for the particles with both phenyl and amino groups may be somewhat lower compared to the particles with only amino groups because of the presence of hydrophobic sites and uneven distribution of the surface charge. In addition, a higher degree of amino group protonation (according to XPS data) results in a higher magnitude of positive charge and zeta potential for the monofunctional sample NH_2-/SiO_2 compared to $NH_2-/C_6H_5-/SiO_2$.

XPS analysis of the samples was conducted to analyze the effect of phenyl groups on the amine ones on the silica surface. The spectra (Figure 2) demonstrated that N 1s can be curve-fitted with two types of nitrogen with expected binding energy (BE): the peaks at lower BE (399.5 eV) is attributed to free amino groups ($-NH_2$) and at higher BE (401.5 eV) is referred to protonated amino groups (NH_3^+).[31,32] According to surface atomic concentrations data (at. %), the peak at 401.5 eV is by 12% smaller for $NH_2-/C_6H_5-/SiO_2$ compared to NH_2-/SiO_2. This may indicate a partially hydrophobic nature of the $NH_2-/C_6H_5-/SiO_2$ particle surface and exclusion of water molecules by phenyl groups. In addition, a higher degree of amino group protonation results in a higher magnitude of positive charge and zeta potential for a monofunctional sample NH_2-/SiO_2 compared to $NH_2-/C_6H_5-/SiO_2$.

The recorded Cu $2p_{3/2}$ spectra of Cu(II) + NH_2-/SiO_2 and Cu(II) + $NH_2-/C_6H_5-/SiO_2$ (Figure 2) were curve-fitted using standard spectra of Cu (0, I, II). The peaks above 942 eV represent the satellite structure formed because of Cu-oxidation, different for Cu II and Cu I, and the intensity of the Cu I satellite is very low in the spectra. Thus, the pronounced peak above 942 eV is just a feature of the whole Cu II peak (main peak + satellite). The curve fitting shows two peaks, at 933.7 and 933.0 eV, matching Cu I and Cu II standards, which can be attributed to Cu(II) and Cu(I) ions, respectively. The Cu(II)/Cu(I) ratios for Cu(II) + NH_2-/SiO_2 and Cu(II) + $NH_2-/C_6H_5-/SiO_2$ are close to 70/30 and 90/10 (Table S2). Apparently, because of the presence of water and sample heating (45 °C) during the spectra recording, a part of Cu^{2+} can be restored (Jurado-López[31] mentioned photo-reduction of copper during XPS measurements). Also, the percent of the recovered metal is higher for Cu(II) + NH_2-/SiO_2, containing more water on the surface (Figure 2). It explains lower zeta potential values of Cu(II) + NH_2-/SiO_2 suspensions compared to Cu(II) + $NH_2-/C_6H_5-/SiO_2$ (Table 2).

These data confirm our assumptions in the article[4,23] that the introduction of hydrophobic groups reduces the number of hydrogen bonds of amino and silanol groups, or between amino groups through water molecules,[33] which improves the

https://dx.doi.org/10.1021/acsomega.0c01335
ACS Omega 2020, 5, 15290−15300

Table 2. Values of pH and Zeta Potential in Function of Suspension Concentration

samples	suspension parameters	suspensions concentration 1%	0.1%	0.01%	0.001%
NH_2-/SiO_2	pH	7.74	7.28	7.20	7.11
	ζ-potential (mV)	28.4	35.8	9.17	−5.2
Cu(II) + NH_2-/SiO_2	pH	6.24	6.76	6.98	7.04
	ζ-potential (mV)	37.1	26.1	0.6	−10.3
$NH_2-/C_6H_5-/SiO_2$	pH	7.91	7.13	7.04	6.93
	ζ-potential (mV)	17.7	25.1	−1.4	−7.2
Cu(II) + $NH_2-/C_6H_5-/SiO_2$	pH	5.74	6.67	6.91	6.96
	ζ-potential (mV)	52.7, 40.3	25.1	−1.2	−8.7

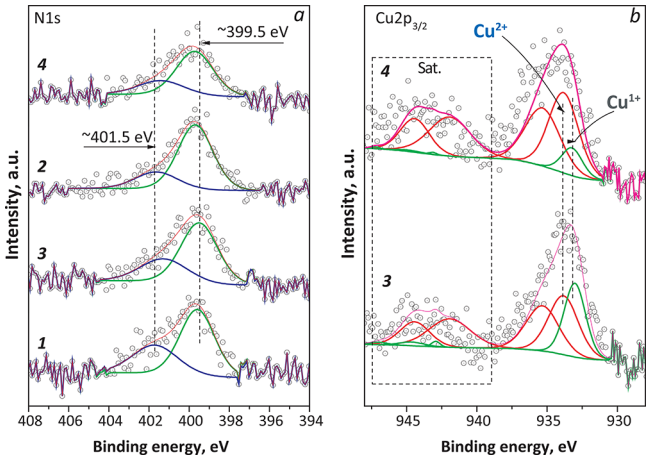

Figure 2. XPS data of N 1s (a) and Cu $2p_{3/2}$ (b) for NH_2-/SiO_2 (1), $NH_2-/C_6H_5-/SiO_2$ (2), Cu(II) + NH_2-/SiO_2 (3), and Cu(II) + $NH_2-/C_6H_5-/SiO_2$ (4).

kinetic characteristics of the bifunctional samples during the adsorption of copper(II) ions from water solutions.[4]

Antibacterial Properties of Amino−/Silica and Amino−/Phenyl−/Silica Particles with and without Adsorbed copper(II) Ions to Gram-Positive Bacteria *S. aureus*. *S. aureus* belongs to Gram-positive bacteria that possess a thick layer of PG in the cell wall and no outer membrane. This very thick PG layer protects Gram-positive bacteria against external stresses, and there is a great variation in the composition and structural arrangement of their PGs.[34] The PG repeat unit of *S. aureus* consists of a disaccharide [*N*-acetyl-glucosamine and *N*-acetyl-muramic acid (NAM)], pentapeptide-stem (L-Ala-D-Glu-L-Lys-D-Ala-D-Ala, with L-Ala attached to NAM of disaccharide), and a bridge structure. The bridge structure in *S. aureus* is a pentaglycine attached to the ε nitrogen of L-Lys in the third position of the stem. A crosslink is formed between the N-terminus of the glycine bridge to the D-Ala (4th position) carbonyl carbon of the adjacent stem. In *S. aureus*, 85 to 90% of the polymerized disaccharides is between 3 and 10 disaccharide units (DU), with an average PG-chain length of only 6 DU.[35] By comparison, other bacteria have much longer average chain lengths ranging from 30 to 60 DU in *E. coli*[36] to over 500 DU in *Bacillus subtilis*.[37] Kim et al.[38] conducted solid-state nuclear magnetic resonance analyses of the cell wall of *S. aureus* showing that PG chains are surprisingly ordered and densely packed because of the short PG chain lengths and high crosslinking degree. The diameter of the PG pores is about 23 Å. Thus, one of the possible mechanisms of antibiotic resistance is size exclusion, when bulky substances are unable to penetrate through the cell wall to reach the cytoplasmic membrane of bacteria.[38]

Different concentrations of Cu^{2+}-loaded and pure NH_2-/SiO_2 and $NH_2-/C_6H_5-/SiO_2$ particles were put in contact with the *S. aureus* cell culture and tested for antimicrobial properties. Here, the mechanism of the antimicrobial effect involves the contact of positively charged particles with negatively charged surfaces of bacterial cells (the zeta potential of *S. aureus* is about −35.0 mV measured at neutral pH[39]). The

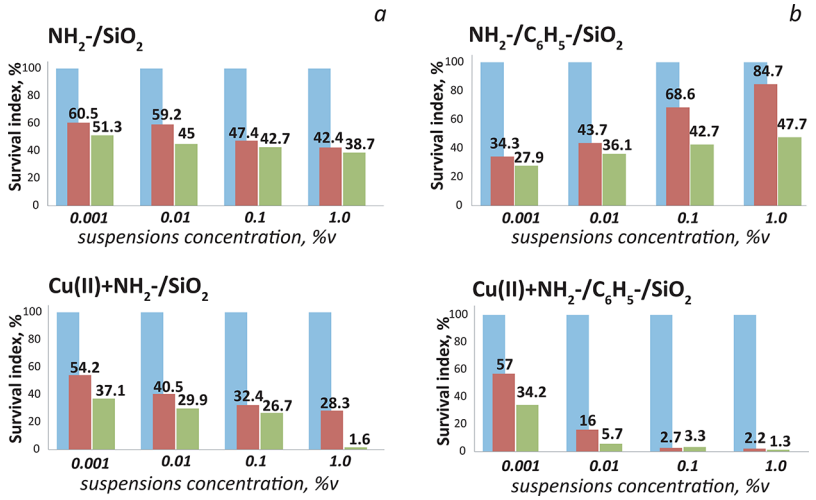

Figure 3. Dependence of the SI for *S. aureus* ATCC 25923 cells on the concentration of the silica particle suspensions and contact time (60 or 120 min) for amino−/silica (a) and amino−/phenyl−/silica (b) samples (blue − control, red − 60 min, green − 120 min).

https://dx.doi.org/10.1021/acsomega.0c01335
ACS Omega 2020, 5, 15290−15300

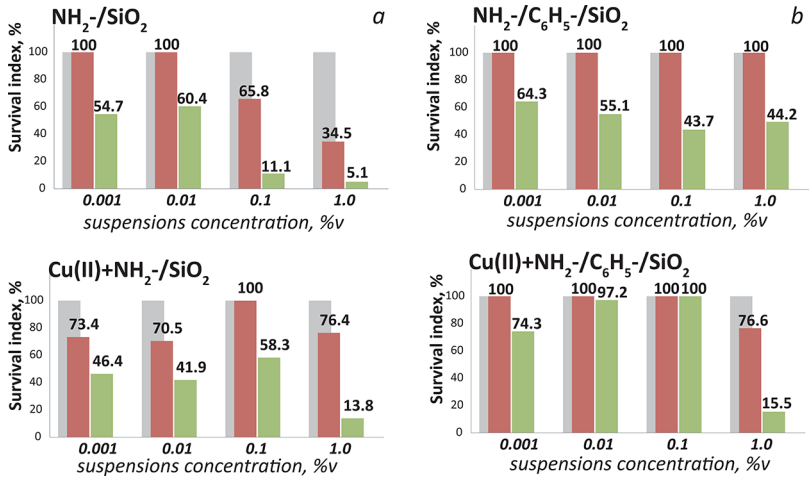

Figure 4. Dependence of the SI for *E. coli* ATCC 25922 cells on the concentration of the silica particle suspensions for amino−/silica (a) and amino−/phenyl−/silica (b) samples (yellow − control, red − 60 min, green − 120 min).

inhibitory effect of NH_2-/SiO_2 on *S. aureus* ATCC 25923 cells (within 60 min of contact) was shown to strengthen with the increasing concentration and contact time. Thus, higher concentrations of NH_2-/SiO_2 (0.1 and 1%) caused a statistically significant decrease in SI to 47.4 and 42.4%, respectively, compared to the control (p = 0.038). A bactericidal effect was less significant at 1−2 order lower concentrations (Figure 3). The prolongation of the contact time of *S. aureus* cells with monofunctional microspheres to 120 min showed statistically significant (p = 0.029) increase in the antibacterial effect by 1.1−1.3 times as compared with the control (Figure 3). It may be explained by the key role of the particle's positive surface charge (zeta potentials +35.8 and +28.4 mV of 1.0 and 0.1% suspensions) in establishing contact with negatively charged bacterial cells (−35 mV) and suppressing their activity. While in the beginning, this charge may be enough, but with the increasing contact time, it may be insufficient to affect new bacterial cells.

Compared to monofunctional NH_2-/SiO_2, bifunctional $NH_2-/C_6H_5-/SiO_2$ microspheres with additional surface phenyl groups revealed the opposite dose dependence of the depressant effect on the concentration at the same exposure time (60 min) (Figure 3). That is, lower concentrations of $NH_2-/C_6H_5-/SiO_2$ showed a stronger *S. aureus* antibacterial effect. Thus, SI of *S. aureus* after contact with 1.0% $NH_2-/C_6H_5-/SiO_2$ was 84.7% and declined (approximately 0.8-fold) with a decrease in concentration showing values of 68.6, 43.7, and 34.3% (Figure 3). Such behavior may be explained by the dependence of antibacterial performance not so much on the particle's zeta potential but on the protonation of amino groups in aqueous environment, observed by Lee at al.[8] by testing silica particles coated with various amine functional polymers. The pH value of 0.001% water suspension of $NH_2-/C_6H_5-/SiO_2$ particles is 6.93, which is more favorable for the protonation of the surface amino groups than pH 7.91 created by 1% water suspension. The two times extension of the contact time of staphylococcal cells with $NH_2-/C_6H_5-/SiO_2$ (to 120 min) was accompanied by increasing the bactericidal effect. In particular, the percentage of surviving *S. aureus* cells decreased 1.8 times at a concentration of 1.0% (SI = 47.7%), 1.6 times at a concentration of 0.1% (SI = 42.7%), and 1.2 times at the concentrations of 0.01 and 0.001% (SI = 36.1 and 27.9%, respectively). Instead, monofunctional NH_2-/SiO_2 microspheres did not exert a similar effect. Thus, confirming previous observations,[4] the introduction of hydrophobic groups in the surface layer of silica particles may increase the number of contact sites between the bacterial cells and the surface of the particles, slowing down the bacterial reproduction.[40]

The inclusion of copper ions into the nanoparticles is one of the most promising strategies for increasing the antibacterial activity of the latter. According to Tsao et al.[41] and Azam et al.,[42] ions of copper can induce changes in the lipid phase of the cytoplasmic membrane of microorganism cells. In addition, copper preparations introduced into the body of mammals in the form of nanoparticles are characterized by prolonged action, lower toxicity compared to salts, the ability to stimulate the microelement regulation mechanisms, and activity of antioxidant enzymes. Because of such characteristics, nanomaterials with introduced copper ions are now considered as promising candidates for creating alternative highly effective antimicrobials. Therefore, we also investigated the activity of silica microspheres with adsorbed Cu^{2+}, Cu(II) + NH_2-/SiO_2, and Cu(II) + $NH_2-/C_6H_5-/SiO_2$ regarding the species of Gram-positive and Gram-negative bacteria.

It was determined that introduction of copper(II) ions into microspheres has significantly improved their activity against the cells of Gram-positive bacteria (Figure 3). So, after the 60 min contact of Cu(II) + NH_2-/SiO_2 with *S. aureus* ATCC 25923 strains, a statistically significant increase in their antibacterial activity was observed compared to NH_2-/SiO_2 at all tested concentrations ($p \leq 0.05$). The number of viable cells decreased with increasing Cu(II) + NH_2-/SiO_2 suspension concentrations: SI values decreased from 54.2 to 40.5 and 32.4% for 0.001, 0.01, and 0.1% suspensions, respectively. Also, they reached the lowest value (SI = 28.3%) at the concentration of 1.0%. Under the conditions of prolongation of the contact of Cu(II) + NH_2-/SiO_2 with staphylococcal cells up to 120 min, the antibacterial activity reached a maximum (Figure 3).

Bactericidal activity of Cu(II) + $NH_2-/C_6H_5-/SiO_2$-type microspheres was more effective than those of Cu(II) + NH_2-/SiO_2. The 60 min contact of staphylococcal cells with Cu(II) + $NH_2-/C_6H_5-/SiO_2$ resulted in a decrease in the number of viable cells (Figure 3) following the dose-dependent pattern. Thus, the SI of staphylococcal cells were 57.0 and

https://dx.doi.org/10.1021/acsomega.0c01335
ACS Omega 2020, 5, 15290−15300

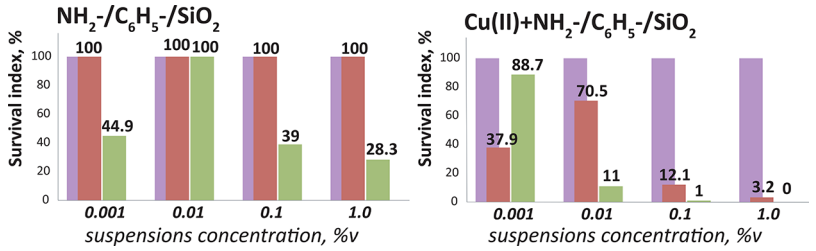

Figure 5. Dependence of the SI for *P. aeruginosa* ATCC 27853 cells on the concentration of the bifunctional silica particle suspensions (purple − control, red − 60 min, green − 120 min).

16.0% at particles concentrations of 0.001 and 0.01%, decreasing to 2.7 and 2.2% with an increasing concentration to 0.1 and 1.0%, respectively. Such antibacterial activity can be explained by the influence of several factors: higher the content of copper(II) ions and zeta potential values, as well as the presence of centers for nonspecific interaction between bacteria and particles, mentioned above for $NH_2-/C_6H_5-/SiO_2$. Besides, the inhibited viability of staphylococcus cells in the presence of copper-containing microspheres may result not only from direct influence of Cu^{2+} but also from the change in the suspension pH (Table 2) because the acidification of the environment (optimal pH is 7.2−7.4) also adversely affects the bacteria growth and reproduction. In addition, according to XPS, materials with adsorbed copper contain both Cu^{+} and Cu^{2+}, which could induce a Fenton-like reaction and enhance the degradation of the microbial cell membrane. Copper antibacterial activity could be attributed to its potential as a catalyst for oxidative damage to tissues through redox transformations between Cu(I) and Cu(II) with the participation of oxygen.[43]

Antibacterial Investigation of the Effect of Amino−/Silica Particles on the SI of Gram-Negative Bacteria *E. coli* and *P. aeruginosa*. Unlike Gram-positive, Gram-negative bacteria along with the cytoplasmic membrane and PG layer possess an outer membrane (consisting of the phospholipid bilayer that contains lipopolysaccharide molecules and proteins).[44] We chose for our study the most well-known species of Gram-negative bacteria *E. coli*[45] and *P. aeruginosa*[46] because they are characterized by natural resistance to antibacterial agents, disinfectants, and other xenobiotics. The reason for this resistance is the low permeability of the outer cell membrane. Investigation of the effect of NH_2-/SiO_2 and $NH_2-/C_6H_5-/SiO_2$ on the cells of representatives of different species of Gram-negative bacteria after 60 min contact made it possible to conclude that compared to staphylococci, NH_2-/SiO_2 microspheres were less effective against Gram-negative bacteria (in particular, *E. coli* ATCC 25922), although the inhibitory activity remained dose-dependent (Figure 4). The SI of *E. coli* cells ranged from 60.9 to 84.5% depending on the concentration ($p \leq 0.05$). Under similar conditions of 60 min contact, the most effective action of $NH_2-/C_6H_5-/SiO_2$ particles against *E. coli* cells was in the concentration of 0.01%. However, there was no statistically significant difference between the effects of different concentrations ($p = 0.3$). Mathelié-Guinlet et al.[7] analyzed the influence of the surface charge and size of silica particles on their antibacterial effect against *E. coli* and reported different mechanisms of action. For pure SiO_2 particles (with negative surface charge), the size is very important. The particles of 50 nm < d < 80 nm were shown to interact through hydrogen bonding with hydroxyl groups of the phospholipid bilayer and thus breaking down the cell clusters. Whereas APTES-modified silica particles (with positive zeta potential) having strong electrostatic affinity to negatively charged *E. coli* cells stick to them inducing drastic damages, such as extra-membrane aggregates and membrane invaginations.

The prolongation of the contact time to 120 min had no visual effect on the antibacterial activity of NH_2-/SiO_2 particles toward *E. coli* cells, whereas $NH_2-/C_6H_5-/SiO_2$ microspheres showed increase in the bactericidal effect (Figure 4). *P. aeruginosa* cells contrary to *E. coli* produce a number of enzymes and are highly resistant to antibiotics.[47] Hence, contrary to *E. coli*, neither monofunctional (NH_2-/SiO_2) nor bifunctional ($NH_2-/C_6H_5-/SiO_2$) microspheres had an inhibitory effect on the cells of the *P. aeruginosa* strain ATCC 27853 during the exposure for 60 min. The absence of the antibacterial effect against *P. aeruginosa* ATCC 27853 can be primarily explained by their natural resistance to antimicrobials[46] because of the low-permeability of the outer membrane in addition to secondary resistance mechanisms, among which systems of active pump-out of antimicrobial agents and xenobiotics play an important role.[47]

The suppressing effect of $NH_2-/C_6H_5-/SiO_2$ bifunctional microspheres on the cells of *P. aeruginosa* strains was indicative (Figure 5). Thus, while during the contact for 60 min, no microbicidal effect was observed, and the extension of the exposure to 120 min allowed registering the inhibition of vitality of *P. aeruginosa* cells. In particular, after the contact with $NH_2-/C_6H_5-/SiO_2$ particle concentration of 0.001% for 120 min, the number of surviving cells, compared with the control, decreased by half, while for concentrations of 1.0 and 0.1%, it was varying within the range of 28.3−39%. Hence, the prolongation of the contact time of $NH_2-/C_6H_5-/SiO_2$ with *P. aeruginosa* resulted in the improvement in their inhibitory activity against Gram-negative bacteria, which was observed for Gram-positive bacteria. It also should be mentioned that such necessity for a longer contact time for $NH_2-/C_6H_5-/SiO_2$ to reveal antibacterial properties may be partially connected with the introduction of phenyl groups. According to Song et al.[40] the BE of bacteria with hydrophobic surfaces is weaker than with hydrophilic. So, on the one side the introduction of phenyl groups increases the portion of free amino groups (contact sites), and they could interact themselves with lipid components of the bacterial membrane, but it also increases the hydrophobicity of the sample. As a result, its antibacterial activity is revealed only during 2 h contact.

The introduction of Cu^{2+} in the composition of microspheres, especially bifunctional, allowed increasing their efficiency against the *P. aeruginosa* cells. Generally, the antibacterial efficiency of Cu^{2+} loaded samples against Gram-negative bacteria appeared lower compared to that against Gram-positive bacteria, although at Cu(II) + $NH_2-/C_6H_5-/$

https://dx.doi.org/10.1021/acsomega.0c01335
ACS Omega 2020, 5, 15290−15300

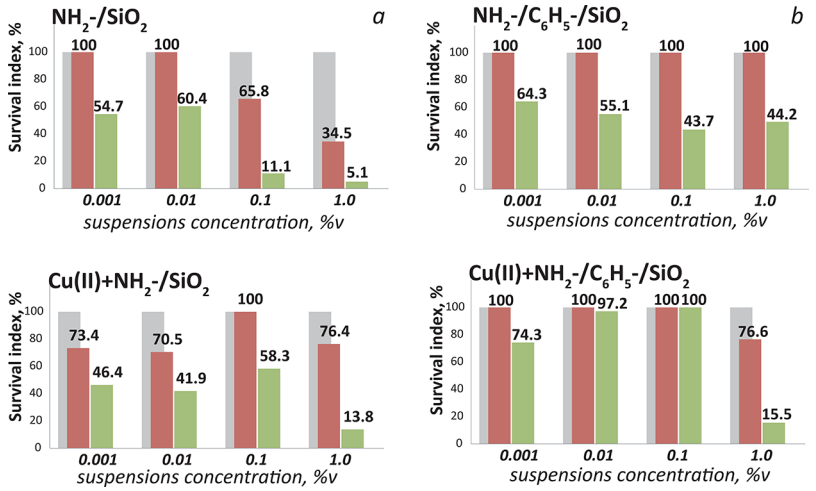

Figure 6. Dependence of the SI for *C. albicans* UCM Y-690 cells on the concentration of the silica particle suspensions for amino−/silica (a) and amino−/phenyl−/silica (b) samples (grey − control, red − 60 min, green − 120 min).

SiO_2 concentrations of 0.1 and 1% and a contact time of 120 min antibacterial activity reached 99 and 100%. Similarly, authors[48] witnessed a bigger diameter of zone of growth inhibition of *S. aureus* when studying the antibacterial activity of copper-doped wollastonite particles against *S. aureus* (Gram-positive) and *E. coli* (Gram-negative) bacterial strains. Theivasanthi and Alagar[49] also showed higher antibacterial activity (18−45% more) of copper nanoparticles against Gram-positive cells of *S. albus*, *S. epidermidis*, and *S. aureus* compared to Gram-negative cells of *E. coli*. Thus, after the contact of Cu(II) + NH_2−/SiO_2 type microspheres with *E. coli* cells for 60 min, similarly to Gram-positive bacteria, a dose-dependent increase in the suppressive effect was observed (Figure 4). When the concentration of Cu(II) + NH_2−/SiO_2 changed from 1.0 to 0.1%, the SI of the *E. coli* cells increased by 21 times. Lowering the particle concentration from 0.1 to 0.01% increased SI of E. coli 2.5 times and from 0.01 to 0.001%—1.3 times.

Similarly to the Cu(II) + NH_2−/SiO_2 microspheres, the antibacterial activity of Cu(II) + NH_2−/C_6H_5−/SiO_2 was found to be significant against the tested Gram-negative cultures and depended on the concentration. Against the cells of the strain *E. coli* ATCC 25922, the most effective of all analyzed Cu(II) + NH_2−/C_6H_5−/SiO_2 concentrations were 1.0 and 0.001%, for which practically no viable cells remained (SI = 0.5 and 0.3%) (Figure 4). Meanwhile, at a concentration of 0.1%, SI was 14.1%, whereas 0.01% had no inhibitory effect on *E. coli*. The latter concentration (0.01%) of Cu(II) + NH_2−/C_6H_5−/SiO_2 microspheres also turned out to be ineffective against *P. aeruginosa* cells ATCC 27853 (SI = 70.5%), whereas other investigated concentrations (1.0, 0.1, and 0.001%), significantly decreased the number of viable cells (SI = 3.2, 12.1, and 37.9%) at a contact time of 60 min.

The prolongation of the influence of Cu(II) + NH_2−/SiO_2 to 120 min almost completely inhibited the viability of *E. coli* cells, except for the 0.01% concentration, which appeared ineffective under these conditions. Significant suppression of the viability of *E. coli* cells was also observed after longer exposure to Cu(II) + NH_2−/C_6H_5−/SiO_2 (Figure 4). The latter sample was also effective against *P. aeruginosa* cells (SI = 1.0 and 11.0% at concentrations of 0.1 and 0.01%, respectively). However, similar to *E. coli* cells, the sensitivity of Pseudomonas cells to the lowest concentration was also negligible (SI = 88.7%).

Thus, as mentioned by other authors,[40] we observe the synergistic effect of phenyl groups and antibacterial properties of silica particles having positive surface charge, hydrophobic groups, and copper(II) ions. These factors altogether lead to the damage of the bacterial cell membranes, violation of their surface charge, disorder of adhesive properties, and subsequent death.

Antifungal Activity of the Samples Against *C. albicans*. Candida species are among the major causes of healthcare-associated infections because they can survive on abiotic surfaces in hospitals.[20] Copper is recognized for its antifungal activity and was shown to possess fungicidal activity against Candida.[20] Therefore, we tested our copper-loaded and copper-free samples against *C. albicans*. Generally, fungicidal activity of copper is somewhat lower compared to its bactericidal activity because of the diverse chemical composition and structural organization of the yeast cell membranes.[20]

Among copper-free samples, only two highest used concentrations of amino−/silica (0.1 and 1.0%) showed an inhibitory effect against *C. albicans* after 60 min contact, SI = 65.8, and 34.5%, respectively ($p \leq 0.01$) (Figure 6). Meanwhile, bifunctional microspheres NH_2−/C_6H_5−/SiO_2 revealed no fungicidal action against *C. albicans* after 60 min contact, similar to Gram-negative cells of *P. aeruginosa*.

Extending the exposure twice allowed increasing the fungicidal action of both monofunctional (NH_2−/SiO_2) and bifunctional (NH_2−/C_6H_5−/SiO_2) microspheres. Similar to the short-term contact, higher concentrations of NH_2−/SiO_2 were the most effective. Thus, at NH_2−/SiO_2 concentrations of 1.0 and 0.1%, the cell SI were 5.1 and 11.1%, respectively ($p \leq 0.026$). No statistically significant difference was found in the case of low NH_2−/SiO_2 suspension concentrations. As for NH_2−/C_6H_5−/SiO_2, they exhibited a fungicidal effect solely in the case of prolongation of the contact (Figure 6). Therefore, in order to ensure the fungicidal action of the microspheres in question, there is a need for longer contact with the eukaryotic yeast cells.

The introduction of Cu^{2+} did not increase significantly the fungicidal activity of neither monofunctional (NH_2−/SiO_2) nor bifunctional (NH_2−/C_6H_5−/SiO_2) microspheres. For both types of microspheres, the statistically significant

https://dx.doi.org/10.1021/acsomega.0c01335
ACS Omega 2020, 5, 15290−15300

fungicidal effect, compared to control (p = 0.032), was observed only at a particle concentration of 1% after 120 min contact (the SI were 13.8 and 15.5%, respectively).

CONCLUSIONS

Two types of samples: monofunctional amino−/silica and bifunctional amino−/phenyl−/silica were synthesized and tested as antimicrobial agents. There were observed obvious advantages of the bifunctional sample already on the stage of characterization. Introduction of the hydrophobic component (phenyl groups) added to the hydrolytic stability of the functional layer. Phenyl groups prevented amino groups from back-bonding, making them available for adsorption; thus, the number of free sites able to interact with bacterial cells increased. Dilution of amino groups with phenyl also promoted simplification of the surface complex with copper(II) ions thus enhancing Cu^{2+} uptake. These advantages, consequently, resulted in improved antimicrobial performance of the bifunctional sample. Thus, the influence of microspheres on the test cultures of microorganisms and the effectiveness of the antimicrobial effect depend on the type of microspheres, their concentration, and the contact time with the cells of microorganisms, as well as taxonomic affiliation of the latter.

Monofunctional silica microspheres with amino groups showed the highest antimicrobial activity in the concentration of 1.0%. The SIs of the bacterial cells after 60 min contact with the particles were as follows: *S. aureus*—42.4%, *E. coli*—60.9%, and *C. albicans*—34.5%. The antibacterial effect of bifunctional silica microspheres with both amino and phenyl groups after 60 min of contact was witnessed only against Gram-positive bacteria. The SI of *S. aureus* after exposure to the lowest of tested concentrations, 0.001%, was 34.3%. Bifunctional silica microspheres (0.1% suspension) demonstrated antimicrobial action against Gram-negative test cultures and a fungicidal effect on microscopic yeast cells only after prolongation of the exposition term to 120 min. The SI of the test strains were: 1.8%—*E. coli*, 39.0%—*P. aeruginosa* and 43.7%—*C. albicans*. The introduction of Cu(II) ions into mono- and bifunctional silica microspheres has dramatically improved their antibacterial and fungicidal activity, which may be due to Fenton-like copper redox cycling resulting in membrane cell oxidation. Owing to the introduction of copper ions, the SI after contact with bifunctional microspheres for 120 min decreased by 36.7 times for *S. aureus*, 5000 times for *E. coli*, 2830 times for *P. aeruginosa*, and 2.9 times for the *C. albicans* strain. Thus, the synthesized materials with copper complexes on the surface can be highly effective disinfectants in sewage treatment.

ASSOCIATED CONTENT

Supporting Information

The Supporting Information is available free of charge at https://pubs.acs.org/doi/10.1021/acsomega.0c01335.

Data on the resistance of cells of test cultures after contact with the adsorbed copper ions on the microsphere surface; XPS data of C 1s, O 1s, Si 2p, N 1s, and Cu $2p_{3/2}$ surface atomic concentrations and binding energies; DRIFT spectra for NH_2-/SiO_2, Cu(II) + NH_2-/SiO_2, $NH_2-/C_6H_5-/SiO_2$, and Cu(II) + $NH_2-/C_6H_5-/SiO_2$; and PCCS particle-size distributions of NH_2-/SiO_2 and $NH_2-/C_6H_5-/SiO_2$ (PDF)

AUTHOR INFORMATION

Corresponding Author

Inna V. Melnyk − *Chuiko Institute of Surface Chemistry of NAS of Ukraine, Kyiv 03164, Ukraine; Institute of Geotechnics, SAS, Kosice 04001, Slovak Republic;* orcid.org/0000-0002-2559-5771; Email: in.melnyk@gmail.com

Authors

Veronika V. Tomina − *Chuiko Institute of Surface Chemistry of NAS of Ukraine, Kyiv 03164, Ukraine*

Iryna M. Furtat − *National University of Kyiv-Mohyla Academy, Kyiv 04070, Ukraine*

Anastasia P. Lebed − *National University of Kyiv-Mohyla Academy, Kyiv 04070, Ukraine*

Sofiya S. Kotsyuda − *Chuiko Institute of Surface Chemistry of NAS of Ukraine, Kyiv 03164, Ukraine; National University of Kyiv-Mohyla Academy, Kyiv 04070, Ukraine*

Hristo Kolev − *Institute of Catalysis BAS, Sofia 1113, Bulgaria*

Maria Kanuchova − *Technical University of Kosice, Kosice 04200, Slovak Republi*

Dominika Marcin Behunova − *Institute of Geotechnics, SAS, Kosice 04001, Slovak Republic*

Miroslava Vaclavikova − *Institute of Geotechnics, SAS, Kosice 04001, Slovak Republic*

Complete contact information is available at: https://pubs.acs.org/10.1021/acsomega.0c01335

Notes

The authors declare no competing financial interest.

ACKNOWLEDGMENTS

The research was funded from the Marie Curie Programme H2020-MSCA-RISE-2016-NANOMED project no. 734641 and the project VEGA 2/0156/19.

REFERENCES

(1) Abd-El-Aziz, A. S.; Agatemor, C.; Etkin, N. Antimicrobial resistance challenged with metal-based antimicrobial macromolecules. *Biomaterials* **2017**, *118*, 27−50.

(2) Regiel-Futyra, A.; Dąbrowski, J. M.; Mazuryk, O.; Śpiewak, K.; Kyzioł, A.; Pucelik, B.; Brindell, M.; Stochel, G. Bioinorganic antimicrobial strategies in the resistance era. *Coord. Chem. Rev.* **2017**, *351*, 76−117.

(3) Braun, K.; Pochert, A.; Lindén, M.; Davoudi, M.; Schmidtchen, A.; Nordström, R.; Malmsten, M. Membrane interactions of mesoporous silica nanoparticles as carriers of antimicrobial peptides. *J. Colloid Interface Sci.* **2016**, *475*, 161−170.

(4) Kotsyuda, S. S.; Tomina, V. V.; Zub, Y. L.; Furtat, I. M.; Lebed, A. P.; Vaclavikova, M.; Melnyk, I. V. Bifunctional silica nanospheres with 3-aminopropyl and phenyl groups. Synthesis approach and prospects of their applications. *Appl. Surf. Sci.* **2017**, *420*, 782−791.

(5) Grumezescu, V.; Andronescu, E.; Holban, A. M.; Socol, G.; Grumezescu, A. M.; Ficai, A.; Lazar, V.; Chifiriuc, M. C.; Trusca, R.; Iordache, F. Fabrication and characterization of functionalized surfaces with 3-aminopropyltrimethoxysilane films for anti-infective therapy applications. *Appl. Surf. Sci.* **2015**, *336*, 401−406.

(6) Song, J.; Kong, H.; Jang, J. Enhanced antibacterial performance of cationic polymer modified silica nanoparticles. *Chem. Commun.* **2009**, *36*, 5418−5420.

(7) Mathelié-Guinlet, M.; Béven, L.; Moroté, F.; Moynet, D.; Grauby-Heywang, C.; Gammoudi, I.; Delville, M.-H.; Cohen-Bouhacina, T. Probing the threshold of membrane damage and cytotoxicity effects induced by silica nanoparticles in Escherichia coli bacteria. *Adv. Colloid Interface Sci.* **2017**, *245*, 81−91.

(8) Lee, I.; Roh, J.; Lee, J.; Song, J.; Jang, J. Antibacterial performance of various amine functional polymers coated silica nanoparticles. *Polymer* **2016**, *83*, 223−229.
(9) Xu, J.; Zhang, Y.; Zhao, Y.; Zou, X. Antibacterial activity of N-halamine decorated mesoporous silica nanoparticles. *J. Phys. Chem. Solid.* **2017**, *108*, 21−24.
(10) Song, J.; Jung, Y.; Lee, I.; Jang, J. Fabrication of pDMAEMA-coated silica nanoparticles and their enhanced antibacterial activity. *J. Colloid Interface Sci.* **2013**, *407*, 205−209.
(11) Gounani, Z.; Asadollahi, M. A.; Meyer, R. L.; Arpanaei, A. Loading of polymyxin B onto anionic mesoporous silica nanoparticles retains antibacterial activity and enhances biocompatibility. *Int. J. Pharm.* **2018**, *537*, 148−161.
(12) Hao, N.; Jayawardana, K. W.; Chen, X.; Yan, M. One-step synthesis of amine-functionalized hollow mesoporous silica nanoparticles as efficient antibacterial and anticancer materials. *ACS Appl. Mater. Interfaces* **2015**, *7*, 1040−1045.
(13) Quang, D. V.; Sarawade, P. B.; Hilonga, A.; Kim, J.-K.; Chai, Y. G.; Kim, S. H.; Ryu, J.-Y.; Kim, H. T. Preparation of amino functionalized silica micro beads by dry method for supporting silver nanoparticles with antibacterial properties. *Colloids Surf., A* **2011**, *389*, 118−126.
(14) Naz, A.; Arun, S.; Narvi, S. S.; Alam, M. S.; Singh, A.; Bhartiya, P.; Dutta, P. K. Cu(II)-carboxymethyl chitosan-silane schiff base complex grafted on nano silica: Structural evolution, antibacterial performance and dye degradation ability. *Int. J. Biol. Macromol.* **2018**, *110*, 215−226.
(15) Tahmasbi, L.; Sedaghat, T.; Motamedi, H.; Kooti, M. Mesoporous silica nanoparticles supported copper(II) and nickel(II) Schiff base complexes: Synthesis, characterization, antibacterial activity and enzyme immobilization. *J. Solid State Chem.* **2018**, *258*, 517−525.
(16) Sportelli, M. C.; Picca, R. A.; Cioffi, N. Nano-antimicrobials based on metals. In *Novel Antimicrobial Agents and Strategies*; Phoenix, D. A., Harris, F., Dennison, S. R., Eds.; Wiley-VCH Verlag GmbH & Co. KGaA, 2014; Vol. *8*, pp 181−218.
(17) Vincent, M.; Hartemann, P.; Engels-Deutsch, M. Antimicrobial applications of copper. *Int. J. Hyg Environ. Health* **2016**, *219*, 585−591.
(18) Aktan, E.; Gündüzalp, A. B.; Özmen, Ü. Ö. Structural, physicochemical characterization, theoretical studies of carboxamides and their Cu(II), Zn(II) complexes having antibacterial activities against E. Coli. *J. Mol. Struct.* **2017**, *1128*, 775−784.
(19) Gritsch, L.; Lovell, C.; Goldmann, W. H.; Boccaccini, A. R. Fabrication and characterization of copper(II)-chitosan complexes as antibiotic-free antibacterial biomaterial. *Carbohydr. Polym.* **2018**, *179*, 370−378.
(20) Ballo, M. K. S.; Rtimi, S.; Kiwi, J.; Pulgarin, C.; Entenza, J. M.; Bizzini, A. Fungicidal activity of copper-sputtered flexible surfaces under dark and actinic light against azole-resistant Candida albicans and Candida glabrata. *J. Photochem. Photobiol., B* **2017**, *174*, 229−234.
(21) Costerton, J. W.; Ingram, J. M.; Cheng, K. J. Structure and function of the cell envelope of Gram-negative bacteria. *Bacteriol. Rev.* **1974**, *38*, 87−110.
(22) Armentano, I.; Arciola, C. R.; Fortunati, E.; Ferrari, D.; Mattioli, S.; Amoroso, C. F.; Rizzo, J.; Kenny, J. M.; Imbriani, M.; Visai, L. The interaction of bacteria with engineered nanostructured polymeric materials: a review. *Sci. World J.* **2014**, *2014*, 410423.
(23) Tomina, V. V.; Melnyk, I. V.; Zub, Y. L.; Kareiva, A.; Vaclavikova, M.; Seisenbaeva, G. A.; Kessler, V. G. Tailoring bifunctional hybrid organic−inorganic nanoadsorbents by the choice of functional layer composition probed by adsorption of Cu^{2+} ions. *Beilstein J. Nanotechnol.* **2017**, *8*, 334−347.
(24) Shirley, D. A. High-resolution X-ray photoemission spectrum of the valence bands of gold. *Phys. Rev. B* **1972**, *5*, 4709−4714.
(25) Scofield, J. H. Hartree-Slater subshell photoionization cross-sections at 1254 and 1487 eV. *J. Electron Spectrosc. Relat. Phenom.* **1976**, *8*, 129−137.
(26) NSAI Standards. *Chemical Disinfectants and Antiseptics: Quantitative Suspension Test for the Evaluation of Fungicidal Activity for Instruments Used in Medical Area: Test Method and Requirements (Phase 2, Step 1)*; European Committee for Standardization: Brussels, 2003, EN 13624.
(27) Glantz, S. A. *Primer of Biostatistics*, 7th ed., ISBN-13:978-0071781503; McGraw-Hill Education/Medical, 2011; p 320.
(28) Sutton, S. Accuracy of plate counts. *J. Validation Technol.* **2011**, *17*, 42−46.
(29) Melnyk, I. Aminosilica nano- and submicrospheres: analysis of factors influencing morphology, structure and properties. *Chem. J. Mold.* **2014**, *9*, 123−127.
(30) Brinker, C. J. Hydrolysis and condensation of silicates: effects on structure. *J. Non-Cryst. Solids* **1988**, *100*, 31−50.
(31) Jurado-López, B.; Vieira, R. S.; Rabelo, R. B.; Beppu, M. M.; Casado, J.; Rodríguez-Castellón, E. Formation of complexes between functionalized chitosan membranes and copper: A study by angle resolved XPS. *Mater. Chem. Phys.* **2017**, *185*, 152−161.
(32) Vieira, R. S.; Oliveira, M. L. M.; Guibal, E.; Rodríguez-Castellón, E.; Beppu, M. M. Copper, mercury and chromium adsorption on natural and crosslinked chitosan films: An XPS investigation of mechanism. *Colloids Surf., A* **2011**, *374*, 108−114.
(33) Zub, Y. L.; Melnyk, I. V.; White, M. G.; Alonso, B. Structural features of surface layers of bifunctional polysiloxane xerogels containing 3-aminopropyl groups and 3-mercaptopropyl groups. *Ads. Sci. Technol.* **2008**, *26*, 119−133.
(34) Schleifer, K. H.; Kandler, O. Peptidoglycan types of bacterial cell walls and their taxonomic implications. *Bacteriol. Rev.* **1972**, *36*, 407−477.
(35) Boneca, I. G.; Huang, Z.-H.; Gage, D. A.; Tomasz, A. Characterization of Staphylococcus aureus cell wall glycan strands, evidence for a new β-N-acetylglucosaminidase activity. *J. Biol. Chem.* **2000**, *275*, 9910−9918.
(36) Glauner, B.; Höltje, J. V. Growth pattern of the murein sacculus of Escherichia coli. *J. Biol. Chem.* **1990**, *265*, 18988−18996.
(37) Hayhurst, E. J.; Kailas, L.; Hobbs, J. K.; Foster, S. J. Cell wall peptidoglycan architecture in Bacillus subtilis. *Proc. Natl. Acad. Sci. U. S. A.* **2008**, *105*, 14603−14608.
(38) Kim, S. J.; Chang, J.; Singh, M. Peptidoglycan architecture of Gram-positive bacteria by solid-state NMR. *Biochim. Biophys. Acta, Biomembr.* **2015**, *1848*, 350−362.
(39) Kłodzińska, E.; Szumski, M.; Dziubakiewicz, E.; Hrynkiewicz, K.; Skwarek, E.; Janusz, W.; Buszewski, B. Effect of zeta potential value on bacterial behavior during electrophoretic separation. *Electrophoresis* **2010**, *31*, 1590−1596.
(40) Song, J.; Kong, H.; Jang, J. Bacterial adhesion inhibition of the quaternary ammonium functionalized silica nanoparticles. *Colloids Surf., B* **2011**, *82*, 651−656.
(41) Tsao, N.; Luh, T.-Y.; Chou, C.-K.; Chang, T.-Y.; Wu, J.-J.; Liu, C.-C.; Lei, H.-Y. In vitro action of carboxyfullerene. *J. Antimicrob. Chemother.* **2002**, *49*, 641−649.
(42) Azam, A.; Ahmed, A. S.; Oves, M.; Khan, M.; Memic, A. Size-dependent antimicrobial properties of CuO nanoparticles against Gram-positive and -negative bacterial strains. *Int. J. Nanomed.* **2012**, *7*, 3527−3535.
(43) Pham, A. N.; Xing, G.; Miller, C. J.; Waite, T. D. Fenton-like copper redox chemistry revisited: Hydrogen peroxide and superoxide mediation of copper-catalyzed oxidant production. *J. Catal.* **2013**, *301*, 54−64.
(44) Miller, S. I.; Salama, N. R. The gram-negative bacterial periplasm: Size matters. *PLoS Biol.* **2018**, *16*, No. e2004935.
(45) Jang, J.; Hur, H.-G.; Sadowsky, M. J.; Byappanahalli, M. N.; Yan, T.; Ishii, S. Environmental Escherichia coli: ecology and public health implications-a review. *J. Appl. Microbiol.* **2017**, *123*, 570−581.
(46) Chatterjee, M.; Anju, C. P.; Biswas, L.; Anil Kumar, V.; Gopi Mohan, C.; Biswas, R. Antibiotic resistance in Pseudomonas aeruginosa and alternative therapeutic options. *Int. J. Med. Microbiol.* **2016**, *306*, 48−58.

https://dx.doi.org/10.1021/acsomega.0c01335
ACS Omega 2020, 5, 15290−15300

(47) Schweizer, H. P. Efflux as a mechanism of resistance to antimicrobials in Pseudomonas aeruginosa and related bacteria: unanswered questions. *Genet. Mol. Res.* **2003**, *2*, 48−62.
(48) Azeena, S.; Subhapradha, N.; Selvamurugan, N.; Narayan, S.; Srinivasan, N.; Murugesan, R.; Chung, T. W.; Moorthi, A. Antibacterial activity of agricultural waste derived wollastonite doped with copper for bone tissue engineering. *Mater. Sci. Eng., C* **2017**, *71*, 1156−1165.
(49) Theivasanthi, T.; Alagar, M. Studies of Copper Nanoparticles Effects on Micro-organisms. *Ann. Biol. Res.* **2011**, *2*, 368−373.

https://dx.doi.org/10.1021/acsomega.0c01335
ACS Omega 2020, 5, 15290−15300